SLAS Discovery 29 (2024) 100195

Contents lists available at ScienceDirect

SLAS Discovery

journal homepage: www.elsevier.com/locate/slasd

Full Length Article

Varieties of interactions of anti-CD133 aptamers with cell cultures from patient glioblastoma

Olga Antipova [a,b,1], Valeria Moiseenko [a,b,1], Fatima Dzarieva [c], Ekaterina Savchenko [b], Igor Pronin [b], Galina Pavlova [b,c], Alexey Kopylov [a,b,*]

[a] Lomonosov Moscow State University, Moscow, Russia
[b] N.N. Burdenko National Medical Research Center of Neurosurgery, Ministry of Health, Moscow, Russia
[c] Institute of Higher Nervous Activity and Neurophysiology, Russian Academy of Sciences, Moscow, Russia

ARTICLE INFO

Keywords:
CD133
Aptamer
Flow cytometry
Glioblastoma
Continuous cell cultures

Development of aptatheranostics for glioblastoma (GB) requires investigating aptamer interactions with cells. The paper has described flow cytometry (FC) assessment of direct interactions of fluorescent anti-CD133 aptamers with cells, focusing on cell cultures derived from patient GB (CCPGB). Conventional cell lines with different levels of CD133 mRNA, Caco-2 and HCT116, were used to compare interactions with known 2′FY-RNA aptamer A15 and DNA aptamers of Ap and Cs series, labeled with FAM and Cy5. In addition, interactions of certain non-aptameric oligonucleotides were studied. In the case of antibody interactions with cells, FC signals, mean fluorescence intensities (MFIs), correlated with sizable amounts of CD133 mRNA in Caco-2 cells, and CCPGBs 107 and G01. Unexpectedly, MFI *per se* could not be the solid indicator of specific interactions of aptamer - CD133/cell. Instead, two types of interactions, target CD133-driven and off-target membrane-associated ones, contribute to MFI. The latter was notably observed for CCPGB Sus/fP2 with tiny CD133 mRNA amount. To prove specificity of aptamer - CD133/cell interactions, titration experiments have been performed, revealing half-saturation concentrations of 120±27 for 2′FY-RNA A15 and 180±12 for DNA Cs5 with Caco-2 cells. This knowledge is an essential step to develop aptatheranostics for GB.

1. Introduction

Glioblastoma multiform (GB) is an aggressive brain tumor with poor prognosis. The current treatment protocol, Stupp Regimen, includes surgery, radiation therapy, temozolomide chemotherapy [1] which provides about a year of patient survival [2]. Efficiency of GB treatment is hindered by infiltrative nature, population heterogeneity, including GB stem-like cells (GSC) [3], genetic and metabolic variations [4], cellular plasticity [5], and propensity for genetic mutations. Post-treatment GSC remnants have tumorigenesis potential [6] leading to recurrence [7]. The GSC marker CD133 has garnered significant attention [8,9]. Novel strategies, like multifunctional drug delivery systems targeted by Molecular Recognition Elements (MoREs), are needed [10]. Despite the limitations of antibodies - poor localization, penetration, and accumulation [11] immunotheranostics is an intensively developing area. To address these challenges, the development of alternative MoREs, like artificial `scaffold' proteins [12], is in progress.

Aptamers, nucleic acid-based `chemical antibodies,' offer a promising solution, addressing issues related to synthesis reproducibility, size, stability, low immunogenicity [13,14]. Advances in targeting CSCs with aptamers have been reported [15]. Anti-CD133 SELEX has been performed on whole cells overexpressing CD133 (Cell-SELEX). The composition of cellular membrane complicates interactions of aptamers with membrane proteins on cells [15], not to mention the challenges posed by endocytosis.

Comparing the properties of already discovered aptamers is crucial, because of differences in application conditions. First attempts have been made [16]. Aptamer Consortium is working on recommendations to uniform that matter [17]. Therefore, aptamer validation remains essential. Flow cytometry (FC) is a preferred method for studying aptamer interactions with cells. Besides, for cancer research it is crucial to apply unique continuous cell cultures from patient GB (CCPGBs). Two hundred publications have described the application of FC for CD133 study of GB cells, with only a few addressing the use of aptamers, and none focusing on CCPGB. It is worth mentioning, that the translation of aptamers into biomedicine strictly confines experimental conditions,

* Corresponding author at: Moscow State University, Leninskie Gory, 1, Moscow, 119991, Russia.
E-mail address: kopylov@belozersky.msu.ru (A. Kopylov).
[1] These authors contributed equally

https://doi.org/10.1016/j.slasd.2024.100195
Received 22 August 2024; Received in revised form 20 October 2024; Accepted 7 November 2024
Available online 17 November 2024

like avoiding extra competitors, contrary to routine aptamer research that focuses on measuring affinity and specificity [15,17].

The paper has described FC to analyze direct interactions of fluorescent 2′FY-RNA aptamer A15 [18], DNA aptamers of Cs [19] and Ap series [20] with cells, reference colorectal cancer cell lines Caco-2, HCT116, and original CCPGBs 107, G01, and Sus/fP2 [21]. For fluorescent antibodies, mean fluorescent intensities (MFIs) correlated with CD133 mRNA amounts for Caco-2 cells and CCPGBs 107, G01, revealing population heterogeneities for CCPGBs. More complex patterns were revealed with fluorescent aptamers. We suggest that MFI is a result of two types of interactions: CD133-driven and membrane-associated. When CD133 mRNA amounts are high, MFI reflects mainly aptamer-CD133 interactions. If CD133 mRNA amounts are low, membrane-associated events dominate, leading to varied MFI patterns. Therefore, MFI *per se* could not indicate CD133 existence on a cell surface; only titration experiments could certify specific binding. The acquired knowledge is crucial for future studies of CCPGBs pursuing translation of aptatheranostics, and more general - therapeutic nucleic acids, into biomedicine.

2. Materials and methods

Aptamer nucleotide sequences are listed in Table 1. Chromatographically pure oligonucleotides were purchased from GenTerra Ltd. (Russia). Aptamers, labeled with either 5′-FAM or 5′-Cy5, were prepared in Dulbecco phosphate buffer saline (DPBS, PanEco Ltd, Russia), containing 10 mM KCl, 5 mM $MgCl_2$. Refolding was performed by heating to 95 °C for 5 min, followed by cooling to room temperature.

Anti-human CD133 APC-conjugated antibodies (Clone No W6B3C1, E-AB-F1268E, isotype - mouse IgG1) for flow cytometry were purchased from Elabscience Biotechnology Inc. (USA). Salmon DNA was sourced from Sigma-Aldrich (USA), sounded, and stored frozen. Yeast tRNA was obtained from Invitrogen (USA).

Human colorectal adenocarcinoma cell line Caco-2 (HTB-37 - ATCC) was purchased from Avtsyn Research Institute of Human Morphology of "Petrovsky National Research centre of Surgery" (Moscow, Russia). Cells were grown in RPMI growth medium with sodium pyruvate (PanEco Ltd., Russia) supplemented with 10% fetal calf serum (FCS), 1% HEPES, 1% GlutaMAX and 1% streptomycin (all Invitrogen, USA); at 37 °C in a 5% CO_2 atmosphere.

Human colon cancer cell line HCT 116 (CCL-247 - ATCC) was purchased from the Russian collection of cell cultures of the Institute of Cytology of the Russian Academy of Sciences (St. Petersburg, Russia). Cells were grown and maintained in culture using Dulbecco's Modified Eagle Medium DMEM (PanEco Ltd., Russia) supplemented with 10% FCS, 1% HEPES, 1% GlutaMAX and 1% streptomycin (all Invitrogen, USA); at 37 °C in 5% CO_2.

Continuous cell cultures derived from surgical samples of patient GB, 107, G01, Sus/fP2 [21] were developed in the Laboratory of Neurogenetics of the N.N. Burdenko Research Institute of Neurosurgery (Moscow, Russia). Cells were grown and maintained in culture using DMEM/F12 with sodium pyruvate (Servicebio, China) supplemented with 10% FCS, 1% HEPES, 1% GlutaMAX and 1% streptomycin (all Invitrogen, USA); at 37 °C in a 5% CO_2 atmosphere.

Cells were maintained for fewer than 3–7 passages after thawing; and 1.5 million cells were seeded for experiments.

2.1. Flow cytometry monitoring of fluorescent antibody and aptamers interactions with cells

Cells were harvested at 80% confluence and trypsinized with 1 ml of 0.25% trypsin-EDTA (PanEco Ltd, Russia). After centrifugation at 1000 g for 3 min, cells were resuspended in DPBS, 5 mM $MgCl_2$, and counted. Cells were spun down and resuspended in growth media with 10% FCS and 10^6/ml incubated at 37 °C for 1 hr for surface regeneration.

Anti-CD133 APC-conjugated antibodies were diluted 1:50 in growth media with 10% FCS and incubated with the cells for 1 h at room temperature in the dark. Cells were washed three times with DPBS containing 5 mM $MgCl_2$, resuspended in 300 µl DPBS with 5 mM $MgCl_2$, and analyzed by flow cytometry. Fluorescent aptamers (1 µM) in a 50% DPBS with 5 mM $MgCl_2$ and 50% growth media with 10% FCS were incubated with cells for 30 min at room temperature in the dark. Cells were washed three times with DPBS, 5 mM $MgCl_2$, resuspended in 300 µl DPBS, 5 mM $MgCl_2$, and subjected to flow cytometry.

The binding affinity of Cy-5-aptamers was analyzed by FC using 5×10^5 Caco-2 cells with various concentrations of aptamers. Aptamer interactions was performed at 25 °C for 30 min with aptamers at concentrations of 0.03, 0.07, 0.13, 0.25, 0.5, and 1 µM in 50% DPBS, 5 mM $MgCl_2$ and 50% growth medium with 10% FCS. The non-aptameric oligonucleotides 2′FY-RNA NARO and DNA dT_{20} at concentrations of 0.03, 0.07, 0.13, 0.25, 0.5, 0.75 and 1 µM were used as controls and incubated with Caco-2 cells in the same mixture of 50% DPBS, 5 mM $MgCl_2$ and 50% growth medium with 10% FCS. After 30 min of incubation in the dark, cells were washed three times with the buffer, resuspended in 300 µl of DPBS, 5 mM $MgCl_2$ and submitted to FC.

Fluorescence intensity was measured with CytoFlex (Beckman Coulter, USA), with 30,000 events collected and analyzed by instrument's software. Data were processed using FlowJo v10.6.2 (FlowJo LCC, USA). Intact cells were identified using FSC-H *vs* SSC-H plot. Results were presented as histograms [22]. Affinity of oligonucleotides to cells was determined as described earlier [18], mean fluorescence intensity (MFI) of intact cells was subtracted from MFI cells incubated with oligonucleotides.

2.2. Statistical analysis

Statistical analyses were performed using Statistica 6.1 (StatSoft, USA). Data are presented as means ± standard deviation of at least three independent experiments, *p*-value of less than 0.05 was considered statistically significant.

Table 1
Nucleotide sequences of aptamers and oligonucleotides.

N	Name	Nucleotide Sequence, 5′-3′*	Length, nt
1	A15	fCfCfCfUfCfCfUrAfCrAfUrArGrGrG	15
2	Cs1	ATTGCACCACAGATTGTTATTATTTAGTTTATCTCCTAGTTTAGATAGTAAGTGCAAT	58
3	Cs5	TTACATCGAGTGGCTTATAAAGTAGGCGTAGGGCTAGGCGGAGAGATGTAA	51
4	Ap1M	TACCAGTGCCGTTTCCCCGGAGGGTCACCCCTGACGCATTCGGTTGAC	48
5	Ap2	TACCAGTGCGATGCTCAGGTGTGCGCCGCCCCGGCGTCCCCGACCAATGCTATCGCCACTGACGCATTCGGTTGAC	76
6	NADO**	CATTTAGGACCAACACAA	18
7	NARO***	rGfCfUrArArGfCfUrGfUfCfCfUfCfCrG	16
8	dT_{20}	TTTTTTTTTTTTTTTTTTTT	20

* r – ribo-, f - 2′-fluordeoxyribo- (2′F-).
** NADO - non-aptameric DNA oligonucleotide.
*** NARO - non-aptameric 2′FY-RNA oligonucleotide.

3. Results

3.1. Antibodies

To standardize FC experiments, interactions of allophycocyanin conjugated mouse anti-human CD133 antibody with conventional Caco-2 cells, having high CD133 mRNA amounts, were tested. On the other hand, CCPGBs have variety of CD133 mRNA levels (Supplementary Fig. S1). Before FC, cells were incubated with antibody for 1 h at room temperature in the dark. Three scenarios are shown in Fig. 1. First, for Caco-2 cells antibody revealed homogeneous population with right shifted MFI (Fig. 1A). Second, for CCPGBs 107 and G01 histograms indicated heterogeneity (Fig. 1D, G), due to cell populations with different CD133 abundance. Third, for CCPGB Sus/fP2, having tiny CD133 mRNA amount, there is no shift (Fig. 1J).

3.2. 2′FY-RNA aptamer Cy5-A15

Well-known 2′FY-RNA aptamer Cy5-A15 [18] has 2′-hydroxyl group of pyrimidine nucleotides substituted with fluorine. Non-aptameric 2′FY-RNA oligonucleotide, Cy5-NARO, was used to reveal off-target interactions. A 1 μM aptamer concentration is high enough [23] to level out binding conditions for cells with different CD133 mRNA amounts. Binding was performed at room temperature for 30 min without competitors/blockers, like extra nucleic acids (using competitors shown at Supplementary Fig. S3). The 2′FY-RNA aptamer A15 was found to be not-toxic to cells (Supplementary Fig. S4).

Three types of MFI shifts were observed. For Caco-2 cells with high CD133 mRNA amount, MFI shift for Cy5-A15 is bigger than for Cy-5-NARO (Fig. 1B, C). Similar trends were observed for CCPGBs, except Sus/fP2. For CCPGB 107, having lower CD133 mRNA amount than Caco-2 (Supplementary Fig. S2), Cy5-A15 gave asymmetrical peak (Fig. 1F). For CCPGB G01, having intermediate CD133 mRNA amount (Supplementary Fig. S2), Cy5-A15 gave symmetrical peak but further right (Fig. 1I). Finally, CCPGB Sus/fP2, with tiny CD133 mRNA amount, MFIs for Cy5-A15 and NARO were the same, and alike for CCPGB G01 (Fig. 1L). The data on APC-labeled antibody binding to CD133 on cells summarized into histograms, which are shown on the right of the flow cytometry results. For the heterogeneous population 107 after incubation with antibodies APC-positive cells signal is shown in the histogram; this population is highlighted in the shaded area in the original flow cytometry graph.

For the sample G01 it was hard to evaluate the amount of a separate population of APC+ G01 cells; therefore the histogram for G01 shows the average signal value without separation into CD133-positive and CD133-negative cells.

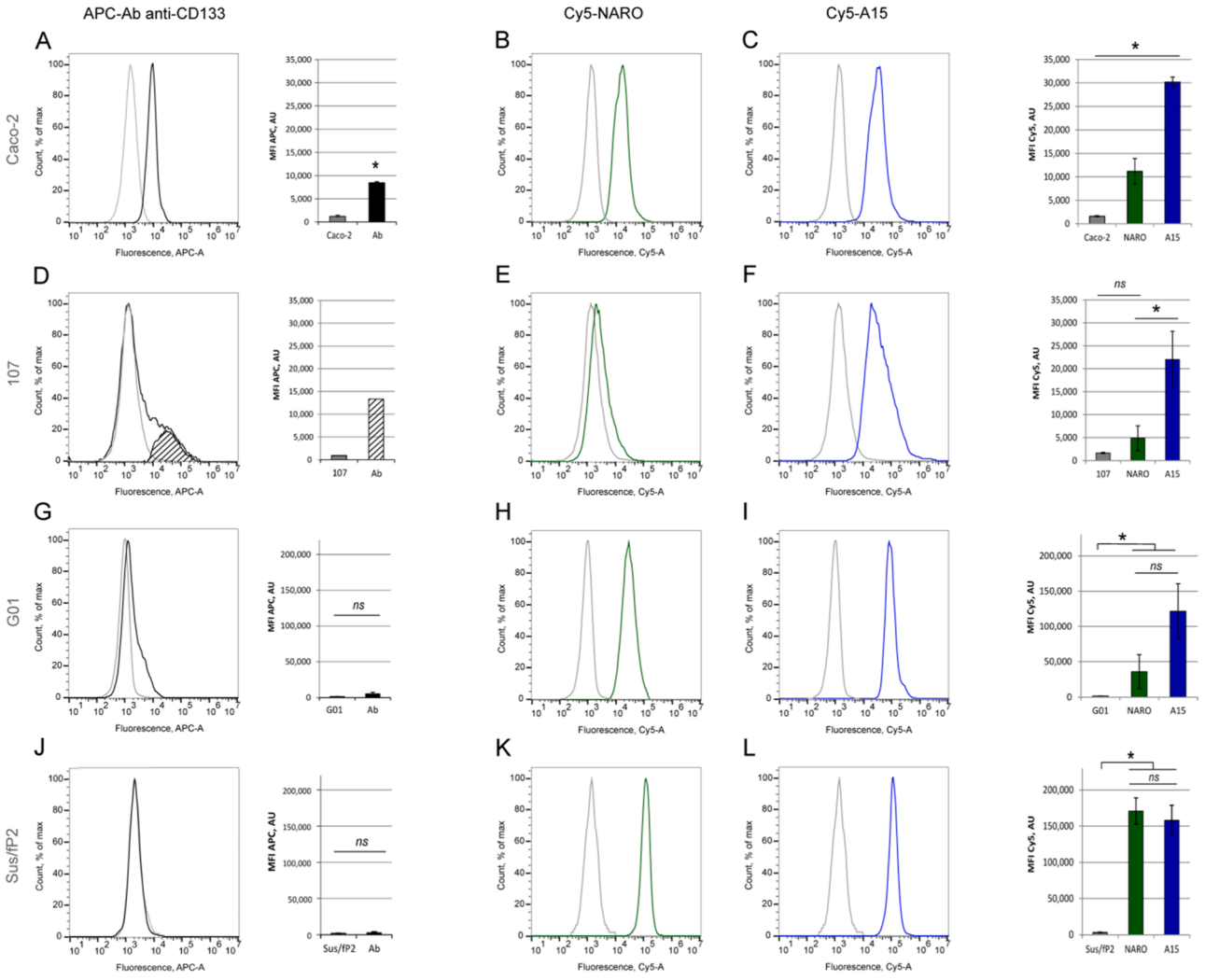

Fig. 1. Flow cytometry data for Caco-2 cells (A-C), and CCPGBs 107 (D-F), G01 (G-I), Sus/fP2 (J-L) incubated with anti-CD133 APC-antibody (A, D, G, J), aptamer 2′FY-RNA Cy5-A15, non-aptameric 2′FY-RNA Cy5-NARO (B, E, H, K). The antibody was diluted 1:50 and incubated for 1 hr, or 1 μM oligonucleotide was incubated for 30 min; both: room temperature, dark. The part of heterogeneous population of the sample 107 APC+ is shadowed. Histograms (C, F, I, L) show statistical data: * - $p < 0.05$.

3.3. DNA aptamers Cs and Ap

Members of two series of DNA aptamers: Cs [19] and Ap [20], each with FAM and Cy5 fluorescent labels, were studied. Possible secondary structures of 2′FY-RNA aptamer A15 and DNA aptamers Ap1M, Ap2, Cs1 and Cs5 represented in Supplementary Figure S1. DNA-aptamers were examined against two CD133-positive cells, Caco-2 and HCT116. The cell lines have different CD133 mRNA amounts; for Caco-2 CD133 mRNA amount is an order of magnitude higher [24].

We have tested interactions of FAM-DNA aptamers with cells Caco-2 and HCT116 (Fig. 2, Supplementary Fig. S5). For both cell lines, there were rightward shifts. For Caco-2 cells, MFI values were 3800 au for Ap1M and 4400 au for Cs5 (Fig. 2A, B, D), with no shift observed for non-aptameric oligonucleotide NADO (Fig. 2C, D). MFIs for cells HCT116 were bigger: 6500 au for Ap1M and 5200 au for Cs5 (Fig. 2E, F, H). However, contrary to Caco-2 cells, NADO did slightly interacted with HCT116 cells (Fig. 2G, H). Results for two other family members, Ap2, Cs1, were similar to Ap1M, Cs5, as shown in Supplementary Fig. S5.

More sensitive Cy5-derivatives of Ap1M and Cs5 were tested with Caco-2 cells (Fig. 3A-C). Both aptamers gave MFI rightward shifts: Ap1M showed an MFI of 7400 au, and Cs5 showed 5200 au, compared to Caco-2 cells autofluorescence at 1400 au. Essentially, for CCPGB 107, histograms of interactions with Ap1M and Cs5 aptamers displayed multiplex profiles (Fig. 3D, E).

Binding parameters of aptamers: 2′FY-RNA A15, DNA Cs5, and non-aptameric oligonucleotides: 2′FY-RNA NARO, DNA dT_{20}, were assessed using Caco-2 cells. Plotting MFIs *vs* oligonucleotide concentrations revealed typical binding curves (Fig. 4E, G), proving specific interactions of aptamers A15 and Cs5. Calculated concentrations of half-saturation were 120 ± 27 nM for A15 (Fig. 4E), and 180 ± 12 nM for Cs5 (Fig. 4G). Contrary, interactions of NARO and dT_{20} yielded linear profile, proving non-specific interactions (Fig. 4F, H).

4. Discussion

One of the main directions in the development of targeted cancer therapy is theranostics, a combination of diagnostics and therapy. Immunotheranostics applies antibodies as Molecular Recognition Elements (MoREs) to detect molecular oncomarkers in tumors, and subsequently utilizes antibody-drug conjugates to eradicate targeted cells. A notable and successful example of theranostics is targeting of the EGFR-2 oncomarker [25].

Considering theranostics applications, an intra-heterogeneous tumor could be roughly classified as having different types of cells. Actively proliferating cells has both a high number of cells and a high number of markers *per* cell, as they promote the tumor growth. For the 'hibernating' cancer stem cells (CSC) or glioblastoma stem cells (GSCs), there is no consensus on set of molecular markers yet. Therefore, it is a great value to work out new methods and approaches for theranostics of GSC, including a development of new MoREs, like scaffolds and aptamers. Selecting CD133 as a marker for the current study we understand that both a number of CD133+ cells and a number of CD133 *per* cell could be low, not mentioning transitional expression. Aptatheranostics requires an understanding of direct interactions of aptamers with CD133 on cells. Besides, a progress in theranostics using novel MoREs could help identify novel types of cancer cells, as it was also shown in the present research.

4.1. Antibodies

Our study initiated by using an anti-CD133 allophycocyanin-antibody to study interactions with cells (Fig. 1A, D, G, J). Anti-CD133 APC-labeled antibody clone specific for AC133 epitope [27], have been chosen. CD133 mRNA amounts rather than protein amounts were taken as references. Despite protein amounts seems more reasonable, they yielded variable data due to difference in processing and glycosylation of CD133, antibodies polymorphism, feeding discussions on CD133

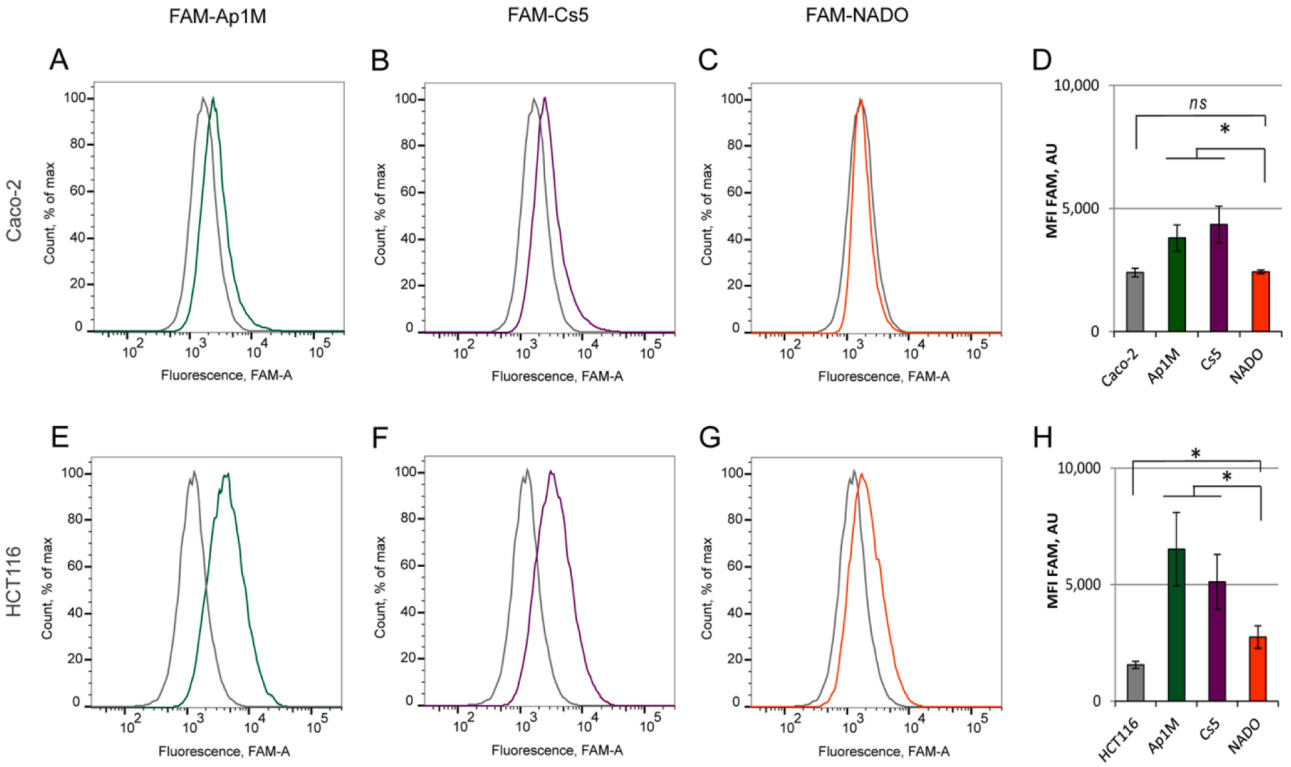

Fig. 2. Flow cytometry data on interactions of cells Caco-2 (A-D) and HCT116 (E-H) with 1 μM FAM-DNA: Ap1M (A, E, D, H), Cs5 (B, F, D, H), NADO (C, G, D, H); room temperature, 30 min, dark. Histograms (D, H) show statistical data, * - $p < 0.05$.

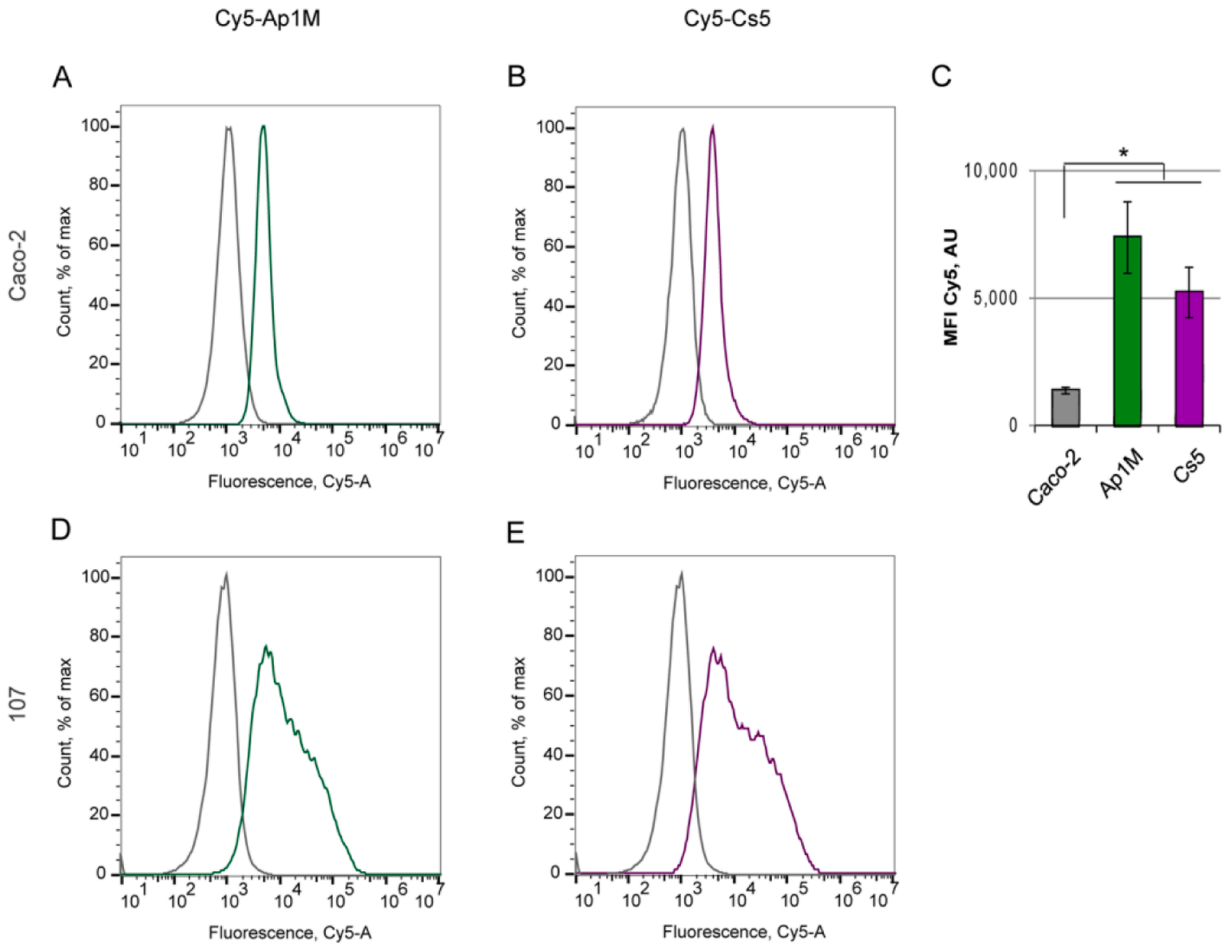

Fig. 3. Flow cytometry data on interactions of cells Caco-2 (A-C), CCPGB 107 (D, E) incubated with 1 μM Cy5-DNA: Cs5 (A, D), Ap1M (B, E); room temperature, 30 min, dark; histogram (C) shows statistical data * - $p < 0.05$.

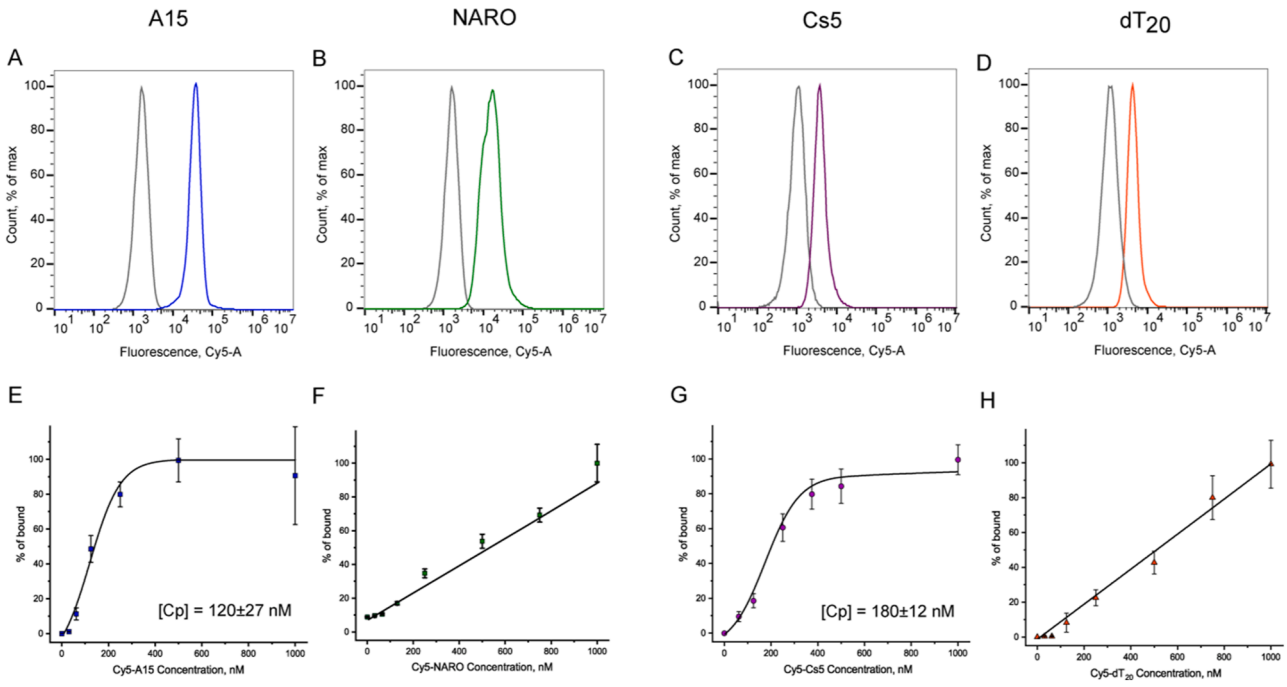

Fig. 4. Flow cytometry data on a titration of cells Caco-2 with Cy5-derivatives: A15 (A), NARO (B), Cs5 (C), dT_{20} (D); 1 μM, room temperature, 30 min, dark. Binding curves: A15 (E), NARO (F), Cs5 (G), dT_{20} (H).

functioning [8,26]. Though CD133 mRNA amounts should not correlate with the protein amounts, for evaluation of interaction scenarios, it could be more relevant.Conventional Caco-2 cells have high CD133 mRNA amount. For CCPGB 107, CD133 mRNA amount was 2.9 times bigger, than for CCPGB G01, and for CCPGB Sus/fP2, CD133 mRNA amount was undetectable (Supplementary Fig. S1). Interactions of antibody with cells Caco-2 gave big MFI shift on FC (Fig. 1A). For CCPGBs 107 and G01, the flow cytometry histograms of anti-CD133 antibody–cells interactions were wide, reflecting intra-tumoral heterogeneity. There were a correlation between CD133 mRNA amounts and MFIs (Fig. 1A, D, G, J). In contrast, CCPGB Sus/fP2, which had very tiny amounts of CD133 mRNA, exhibits no shift in histogram of anibody-cell interactions (Fig. 1J).

4.2. 2′FY-RNA aptamer A15

For aptamer studies, we used commercially available 2′-fluorpyrimidine aptamer A15, known to interact with the glycosylated AC133 epitope (CD133/1) [18]. Unlike most aptamer studies [15,17], we did not pre-block cells with extra nucleic acids, having in mind a translation of aptatheranostics into biomedicine (experiments for blocking Caco-2 cells with nucleic acid pretreatment were described in Supplementary Fig. S3). Direct interactions of aptamer A15 with Caco-2 cells yielded big rightward MFI shift, 30,000 au (Fig. 1C), comparable to shifts of antibody interactions (Cy5-label of aptamers is a fluorescent analog of APC-label of antibodies) (Fig. 1A).

Downgrading CD133 mRNA amount for CCPGB 107, aptamer A15 yielded widened peak with maximum at 22,000 au (Fig. 1F). Further downgrading CD133 mRNA amount for CCPGB G01 led to a narrow peak with unexpectedly significant MFI shift to 150,000 au, (Fig. 1I), which overlaps with right shoulder for CCPGB 107. CD133 mRNA amount of CCPGB 107 indicate tentative threshold value for aptamer A15 flow cytometry detection of target CD133-driven interactions. This value for aptamer A15 (2.9) is higher than the value for antibody (1.0), which could fit with their affinity differences.

CCPGB Sus/fP2, despite tiny CD133 mRNA amount, exhibited the same big MFI, 150,000 au (Fig. 1L). Probably big MFI reflects essential off-target membrane-associated events. Analogous effect was found earlier [28]. Non-aptameric oligonucleotide NARO also interacted with cells, yielding MFIs as roughly one third of aptameric MFIs (Fig. 1E, H, K). It is exception for CCPGB Sus/fP2, having equal MFIs for NARO and aptamer A15 (Fig. 1M), which means a preponderance of non-target membrane-associated events.

Therefore, MFI *per se* does not indicate a presence of CD133 receptor on cells. MFI is generated by interplay of at least two events: target CD133-driven, and off-target membrane-associated. MFIs for second events are governed by cell nature only, with no rules yet. Lack of MFI correlation with tabular CD133 mRNA levels for cell lines HT-29, PLC/PRF/5, and PA-1 was also reported in literature [18], but with no comments. No surprise that for 2′FY-RNA aptamer A15 comparing to antibody, membrane-associated events are more pronounced. A reason could be an increased hydrophobicity of 2′FY-RNA backbone [29]. Therefore, it is worth comparing properties of 2′FY-RNA aptamer with DNA aptamer.

4.3. DNA aptamers series Cs and Ap

Little is known on anti-CD133 DNA aptamers. To gain information comparable with RNA aptamer A15, we tested DNA aptamers Cs [19] and Ap [20] in a similar way. Interactions of FAM-DNA aptamers Ap1M, Cs5 with conventional cell line Caco-2 yielded MFI right shifts (Fig. 2A–D). There was no shift in the case of the control non-aptameric DNA oligonucleotide (NADO, Fig. 2C). Interactions of the DNA-aptamers with HCT116 cell line, despite having lower CD133 mRNA amount, resulted in even bigger rightward shifts, along with widened histograms (Fig. 2E–H), probably due to off-target membrane-associated events. Therefore, an anomalous tendency for DNA aptamers, similar to that we previously observed for 2′FY-RNA aptamer A15, has been sustained despite the differences in the chemical nature of both backbone and fluorescent label. The behavior of NADO is in a vein of this tendency.

Comparing Cy5-labeled DNA aptamers with 2′FY-RNA aptamer A15 (Fig. 1C, F, I, L), we found that DNA aptamers showed lower MFI values with cells Caco-2 and CCPGB 107 (Fig. 3). Understanding all provisos of fluorescence, MFI values for DNA aptamers are less than for 2′FY-RNA aptamer A15, probably due to lower affinities. Nevertheless, like the antibody (Fig. 1D) and unlike 2′FY-RNA aptamer A15 (Fig. 1F), DNA aptamers are more sensitive to heterogeneity of CCPGB 107 (Fig. 3D, E), and hydrophobicity difference could be a reason.

4.4. *Affinities* of fluorescent Cy5 derivatives of 2′FY-RNA aptamer A15, DNA aptamer Cs5, and non-aptameric oligonucleotides NARO and dT_{20} to Caco-2 cell line

The MFI, indicating an amount of bound ligand to a target cell, *per se* does not reveal either affinity or specificity of interactions. Therefore, titration experiments are required. Conventional cell line Caco-2 was titrated with Cy5-labeled aptamers 2′FY-RNA A15, DNA Cs5, and non-aptameric NARO and dT_{20} (Fig. 4). Titration experiments with Cy5-oligonucleotides revealed linear correlations for non-specific binding of NARO and dT_{20} (Fig. 4B, D). Contrary to that, both RNA A15 and DNA Cs5 aptamers showed specific interactions (Fig. 4E, G). The calculated half-saturation concentrations are 120±27 and 180±12 nM, respectively, with RNA aptamer A15 showing slightly more affinity, than DNA aptamer Cs5. Because ‘a cell’ is not ‘a molecule’, we use the term ‘concentration of half-saturation’ instead of K_d. Both aptamers were originally selected against overproducing CD133 cells [18,19]. Published quasi-K_d values align with our findings: 82 nM for cell lines HT−29 [18], and 32 nM for Hep3B [30], having transcription levels 49.7 and 143.2 nTPM, respectively [24]. DNA aptamer Cs5 gave quasi-K_d value 16,3 ± 6,8 [19] for transfected cell line (CHO)-K1 having assumed high CD133 mRNA levels. All data fit with a hypothesis that for cells with low levels of CD133, contribution of off-target membrane-associated interactions are more pronounced, thereby increasing measured concentrations of half-saturation.

In conclusion, the development of aptatheranostics for GB using CCPGBs will face different cases, depending on an aptamer type, CD133 status, and properties of cell membrane. DNA and 2′FY-RNA aptamers interact with cells differently, influenced by enhanced hydrophobicity of 2′FY-RNA. The flow cytometry signal probably is generated by two events: target aptamer interactions with CD133, and off-target membrane-associated events, which are not yet understood. The less CD133 amount cells have, the bigger deposit of membrane-associated effects is. The acquired knowledge is an essential step toward a translation of aptamers into theranostics of GB, and more generally, therapeutic nucleic acids into biomedicine.

Funding information

Research was supported by Ministry of Science and Higher Education of Russian Federation Grant (Agreement No. N°75-15-2024-561, April 24, 2024).

Declaration of competing interest

The authors declare the following financial interests/personal relationships which may be considered as potential competing interests:

Olga Antipova, Valeria Moiseenko, Fatima Dzarieva, Ekaterina Savchenko, Igor Pronin, Galina Pavlova, Alexey Kopylov reports was provided by Ministry of Science and Higher Education of Russian Federation. If there are other authors, they declare that they have no known competing financial interests or personal relationships that could have appeared to influence the work reported in this paper.

Acknowledgments

Authors are grateful to D.V. Shamadykova, S.F. Drozd for help, O.A. Dontsova for suggestions. INSOAP stimulation is appreciated.

Supplementary materials

Supplementary material associated with this article can be found, in the online version, at doi:10.1016/j.slasd.2024.100195.

References

[1] Stupp R, Mason WP, Van Den Bent MJ, Weller M, Fisher B, Taphoorn MJ, Belanger K, Brandes AA, Marosi C, et al. Radiotherapy plus concomitant and adjuvant temozolomide for glioblastoma. N Engl J Med 2005;352:987–96. https://doi.org/10.1056/NEJMoa043330.

[2] Miller KD, Ostrom QT, Kruchko C, Patil N, Tihan T, Cioffi G, Fuchs HE, Waite KA, Jemal A, et al. Brain and other central nervous system tumor statistics. CA Cancer J Clin 2021;71(5):381–406. https://doi.org/10.3322/caac.21693.

[3] Singh SK, Hawkins C, Clarke ID, Squire JA, Bayani J, Hide T, Henkelman RM, Cusimano MD, Dirks PB. Identification of human brain tumour initiating cells. Nature 2004;432(7015):396–401. https://doi.org/10.1038/nature03128.

[4] Innes JA, Lowe AS, Fonseca R, Aley N, El-Hassan T, Lau MCJ, Eddaoudi A, Marino S, Brandner S. Phenotyping clonal populations of glioma stem cell reveals a high degree of plasticity in response to changes of microenvironment. Lab Invest 2022;102(2):172–84. https://doi.org/10.1038/s41374-021-00695-2.

[5] He Y, Døssing KBV, Sloth AB, He X, Rossing M, Kjaer A. Quantitative evaluation of stem-like markers of human glioblastoma using single-Cell RNA sequencing datasets. Cancers (Basel) 2023;15(5):1557. https://doi.org/10.3390/cancers15051557.

[6] Prager BC, Bhargava S, Mahadev V, Hubert CG, Rich JN. Glioblastoma stem cells: driving resilience through chaos. Trends Cancer 2020;6(3):223–35. https://doi.org/10.1016/j.trecan.2020.01.009.

[7] Knudsen AM, Halle B, Cédile O, Burton M, Baun C, Thisgaard H, Anand A, et al. Surgical resection of glioblastomas induces pleiotrophin-mediated self-renewal of glioblastoma stem cells in recurrent tumors. Neuro Oncol 2022;24(7):1074–87. https://doi.org/10.1093/neuonc/noab302.

[8] Kopylov AM, Antipova O, Pavlova GV. Molecular markers of neuro-oncogenesis in patients with glioblastoma. Zh Vopr Neirokhir Im N N Burdenko 2022;86(6):99–105. https://doi.org/10.17116/neiro20228606199.

[9] MacLean MR, Walker OL, Arun RP, Fernando W, Marcato P. Informed by cancer stem cells of solid tumors: advances in treatments targeting tumor-promoting factors and pathways. Int J Mol Sci 2024;25(7):4102. https://doi.org/10.3390/ijms25074102.

[10] Smiley SB, Zarrinmayeh H, Das SK, Pollok KE, Vannier MV, Veronesi MC. Novel therapeutics and drug-delivery approaches in the modulation of glioblastoma stem cell resistance. Ther Deliv 2022;13(4):249–73. https://doi.org/10.4155/tde-2021-0086.

[11] Narsinh KH, Perez E, Haddad AF, Young JS, Savastano L, Villanueva-Meyer JE, Winkler E, de Groot J. Strategies to improve drug delivery across the blood-brain barrier for glioblastoma. Curr Neurol Neurosci Rep 2024;24(5):123–39. https://doi.org/10.1007/s11910-024-01338-x.

[12] Zajc CU, Salzer B, Taft JM, Reddy ST, Lehner M, Traxlmayr MW. Driving CARs with alternative navigation tools - the potential of engineered binding scaffolds. FEBS J 2021;288(7):2103–18. https://doi.org/10.1111/febs.15523.

[13] Bauer M, Strom M, Hammond DS, Shigdar S. Anything you can do, I can do better: can aptamers replace antibodies in clinical diagnostic applications? Molecules 2019;24(23):4377. https://doi.org/10.3390/molecules24234377.

[14] Doherty C, Wilbanks B, Khatua S, Maher 3rd LJ. Aptamers in neuro-oncology: an emerging therapeutic modality. Neuro Oncol 2024;26(1):38–54. https://doi.org/10.1093/neuonc/noad156.

[15] Shigdar S, Agnello L, Fedele M, Camorani S, Cerchia L. Profiling cancer cells by cell-SELEX: use of aptamers for discovery of actionable biomarkers and therapeutic applications thereof. Pharmaceutics 2021;14(1):28. https://doi.org/10.3390/pharmaceutics14010028.

[16] Song X, Yu H, Sullenger C, Gray BP, Yan A, Kelly L, Sullenger B. An aptamer that rapidly internalizes into cancer cells utilizes the transferrin receptor pathway. Cancers (Basel) 2023;15(8):2301. https://doi.org/10.3390/cancers15082301.

[17] McKeague M, Calzada V, Cerchia L, DeRosa M, Heemstra JM, Janjic N, Johnson PE, Kraus L, et al. The minimum aptamer publication standards (MAPS guidelines) for de novo aptamer selection. Aptamers 2022;6:10–8.

[18] Shigdar S, Qiao L, Zhou S-F, Xiang D, Wang T, Li Y, Lim LY, Kong L, Li L, Duan W. RNA aptamers targeting cancer stem cell marker CD133. Cancer Lett 2013;330(1):84–95. https://doi.org/10.1016/j.canlet.2012.11.032.

[19] Li W, Wang Z, Gao T, Sun S, Xu M, Pei R. Selection of CD133-targeted DNA aptamers for the efficient and specific therapy of colorectal cancer. J Mater Chem B 2022;10(12):2057–66. https://doi.org/10.1039/d1tb02729h.

[20] Ge MH, Zhu XH, Shao YM, Wang C, Huang P, Wang Y, Jiang Y, et al. Synthesis and characterization of CD133 targeted aptamer-drug conjugates for precision therapy of anaplastic thyroid cancer. Biomater Sci 2021;9(4):1313–24. https://doi.org/10.1039/d0bm01832e.

[21] Pavlova G, Belyashova A, Savchenko E, Panteleev D, Shamadykova D, Nikolaeva A, Pavlova S, Revishchin A, Golbin D, et al. Reparative properties of human glioblastoma cells after single exposure to a wide range of X-ray doses. Front Oncol 2022;12:912741. https://doi.org/10.3389/fonc.2022.912741.

[22] Nakhjavani M, Giles B, Strom M, Vi C, Attenborough S, Shigdar S. A flow cytometry-based cell surface protein binding assay for assessing selectivity and specificity of an anticancer aptamer. J Vis Exp 2022;187. https://doi.org/10.3791/64304.

[23] Powell Gray B, Song X, Hsu DS, Kratschmer C, Levy M, Barry AP, Sullenger BA. An aptamer for broad cancer targeting and therapy. Cancers (Basel) 2020;12(11):3217. https://doi.org/10.3390/cancers12113217.

[24] The Human Protein Atlas. https://www.proteinatlas.org/ENSG00000007062-PROM1/cell+line, 2024 (accessed 24 Jule 2024).

[25] Siena S, Di Bartolomeo M, Raghav K, Masuishi T, Loupakis F, Kawakami H, et al., DESTINY-CRC01 investigators. Trastuzumab deruxtecan (DS-8201) in patients with HER2-expressing metastatic colorectal cancer (DESTINY-CRC01): a multicentre, open-label, phase 2 trial. Lancet Oncol 2021;22(6):779–89. https://doi.org/10.1016/S1470-2045(21)00086-3.

[26] Moreno-Londoño AP, Robles-Flores M. Functional roles of CD133: more than Stemness associated factor regulated by the microenvironment. Stem Cell Rev Rep 2024;20(1):25–51. https://doi.org/10.1007/s12015-023-10647-6.

[27] Kemper K, Sprick MR, de Bree M, Scopelliti A, Vermeulen L, Hoek M, Zeilstra J, Pals ST, Mehmet H, Stassi G, Medema JP. The AC133 epitope, but not the CD133 protein, is lost upon cancer stem cell differentiation. Cancer Res 2010;70(2):719–29. https://doi.org/10.1158/0008-5472.CAN-09-1820.

[28] Song X, Yu H, Sullenger C, Gray BP, Yan A, Kelly L, Sullenger B. An aptamer that rapidly internalizes into cancer cells utilizes the transferrin receptor pathway. Cancers (Basel) 2023;15(8):2301. https://doi.org/10.3390/cancers15082301.

[29] Shubham S, Hoinka J, Banerjee S, Swanson E, Dillard JA, Lennemann NJ, Przytycka TM, et al. A 2′FY-RNA motif defines an aptamer for ebolavirus secreted protein. Sci Rep 2018;8(1):12373. https://doi.org/10.1038/s41598-018-30590-8.

[30] Duan W. (2014) CD133 aptamers for detection of cancer stem cells. Patent WO 2014/019024 A1, dated 02.08.2012.